Heliyon 6 (2020) e05330

Contents lists available at ScienceDirect

Heliyon

journal homepage: www.cell.com/heliyon

Research article

AU richness within the 5′ coding region of the *Escherichia coli* heat-stable enterotoxin b mRNA affects toxin secretion

Eyad Kinkar, Ayat Kinkar, Mazen Saleh *

Department of Biology, Laurentian University, 935 Ramsey Lake Road, Sudbury P3E 2C6, Canada

ARTICLE INFO

Keywords:
Cell biology
Biochemistry
Microbiology
Genetics
Escherichia coli
Mutation
Site-directed mutagenesis
Protein engineering
Protein folding
Signal peptide
Protein secretion
Heat-stable enterotoxin b
STb
mRNA
AU richness

ABSTRACT

The majority of protein secretion in bacteria is mediated by the T2SS pathway. Substrates processed through this pathway are guided by the N-terminal signal sequence within the nascent polypeptide. Recent experimental evidence suggests that in similar secretory pathways, such as the T3SS, information in the 5′ coding region of the mRNA affects secretion and may also participate in mRNA localization. The majority of studies on the effects of AU richness on translation have focussed on the 5′ UTR in mRNAs. To look at the effects of AU richness within the coding region of mRNA on secretion, we have generated several silent mutations within the 5′ coding region of the *E. coli* heat-stable enterotoxin b (STb). This toxin is a well studied T2SS substrate. The mutations were generated such that AU richness within the 5′ coding region (corresponding to the N-terminal signal sequence) was gradually reduced. Reduction of AU richness within the first 15 codons resulted in reduced secretion of the toxin as the AU/GC ratio was reduced from 2.13 for the WT STb to 1.65 (S-I) and subsequently to 1.30 (S-II). This reduction did not correlate with mRNA accumulation and decreased stability of the transcripts could not account for the reduced secretion observed. Reduction of AU richness beyond the first 15 codons recovered secretion efficiency of the toxin (S-III). To validate the experimental approach, a positive control was used in which a mutation involving the insertion of a positive charge within the hydrophobic domain of the N-terminal signal sequence was constructed. As expected, this mutation abolished secretion of the toxin. In conclusion, reducing AU richness within the 5′coding region in the STb mRNA reduces toxin secretion but other factors, such as formation of hairpins, must also be taken into consideration. This will have implications for both homologous and heterologous expression of STb for biological studies and for toxin production.

1. Introduction

Translation of mRNA in bacteria can be regulated through several mechanisms. These include mRNA stability and its susceptibility to exo- and endonuclease attack, mRNA binding proteins, or conformational masking of the initiation site. Endonucleolytic attack of mRNAs is not random because of the absence of a correlation between the length of mRNA and half-life [1]. Stabilization of mRNA involves specific sequences within the 5′ UTR of the mRNA [2], or presence of stem-loop structures in the 3′ UTR of the mRNA or intercistronic regions [3]. Conformational masking involves presence of stem-loop structures within the ribosome binding site (RBS) of the mRNA [2, 3]. Conformational changes within the mRNA can then unmask this site and initiate translation. Proteins that bind and sequester specific mRNAs bind to their target without affecting mRNA folding. Hairpins normally slow down or inhibit the assembly of the ribosome-mRNA complex as the RBS is masked. Unmasking the RBS may involve specific factors that bind to and unfold the mRNA near the RBS, as in the case of certain regulatory small RNAs, or indirectly by binding to a protein factor. Examples of regulation through binding of an inhibitory RNA have been documented for the bacterial OxyS RNA [4] and the DsrA RNA [5]. An example of the latter mode of regulation, binding of a protein factor, has been reported for the carbon storage regulator A (CsrA), whereby its binding to the target mRNA is inhibited by small RNAs [6].

Protein synthesis efficiency, specifically, can be regulated through codon use. Codons that are rare or certain abundant codons can slow down or enhance translation on the ribosome [4]. Genes with high levels of expression tend to be enriched in codons ending in A/U [4]. This is more evident in the first 18 nucleotides (nt), which are normally shielded within the ribosome during the initiation step. In this region, A increases the probability of high expression but G reduces it [7]. The effects of C and U in this region are intermediate. Control of protein synthesis in this

* Corresponding author.
E-mail address: msaleh@laurentian.ca (M. Saleh).

https://doi.org/10.1016/j.heliyon.2020.e05330
Received 2 April 2020; Received in revised form 29 June 2020; Accepted 20 October 2020

manner is particularly common in polycistronic transcripts and large polypeptides. In the former, slowing down translation has been hypothesized to minimize ribosome collision during translation [8]. In the case of larger polypeptides, particularly those containing separate domains, the slowing down could potentially provide time for the translated regions to fold properly [9]. Slow translating segments have been shown to be particularly enriched in folded proteins destined for secretion through the Tat pathway [9, 10] compared with those secreted in an extended form through the Sec pathway [9, 11]. Then, what about the effects of AU richness in single, not polycistronic transcripts, and not within the 5′ UTR, and that encode for small rather than large proteins? In this case, one can reasonably predict that none of these mechanisms would explain any effects observed in this hypothetical situation.

Effects of codon usage and AU richness on protein translation have been investigated in several proteins but all such studies focussed on cytoplasmic and membrane proteins [12, 13, 14, 15]. Additionally, codon changes in those studies involved segments of the mRNA not involved in targeting the protein product of those transcripts. One study, however involved changes in codons within the 5′ coding region of the mRNA that produces a Type-III secretion system (T3SS) substrate [16]. In that study, Anderson and Schneewind have shown that the mRNA sequence, and not the amino acid sequence, in the T3SS substrate affect targeting for secretion. There are no reports of such effects on a Type-II secretion system (T2SS) substrate. To look at the role that codons and AU richness may play in translation efficiency of a T2SS substrate, we used the *Escherichia. coli* heat-stable enterotoxin b (STb) as a test protein. This toxin is composed of 71 amino acids and contains a cleavable N-terminal signal sequence. Gradual decrease in AU richness within the 5′ coding region of the mRNA was applied in three sub-regions of the secretion signal sequence, separately. The effects of these mutations on secretion efficiency of the toxin and the corresponding levels of their mRNAs were investigated. For purposes of this study, we define secretion efficiency as the ratio of the secreted protein level to the level of its mRNA transcript.

2. Materials and methods

2.1. Materials

The sequence of the *sTb* gene was obtained from the protein data bank (PDB) version 4 (http://www.rcsb.org/pdb/explore/explore.do?structureId=1EHS). The coding region of *sTb* was synthesized by Invitrogen (Thermo Fisher Scientific Inc., Toronto, Canada) in plasmid pDS32. All bacterial culture media and chemicals for gel electrophoresis and Western blots were purchased from Sigma-Aldrich Chemical Co. (Oakville, Canada), unless otherwise indicated. Chemi-competent *E. coli* BL-21 were purchased from Bio-Rad Laboratories (Mississauga, Canada). All plasmids used in this study are identified in Table S1.

2.2. RNA structure simulations

To aid in the analysis of the results, RNA secondary structure simulations were generated using the RNAstructure (17) program at http://rna.urmc.rochester.edu/RNAstructureWeb/ with the following conditions: temperature (K) at 310.15°, maximum loop size of 30, and a window size of 3 [17]. The simulations were generated with the WT and mutants constructs including 29 nucleotides upstream of the start codon to mimic the natural mRNA transcripts that contain the ribosome-binding site.

2.3. Plasmid DNA manipulations

Generally, *E. coli* was cultivated in selective Luria-Bertani (LB) agar plate and liquid medium. The LB contains (10g of Tryptone, 5g of Yeast extract and 10g Sodium chloride per liter) and for plates 15g agar was added to give a 1.5% (w/v) per liter final concentration. Media were prepared with 100 μg/ml Ampicillin (Amp) for selection. The pD444-SR, an expression vector from DNA2.0 (Menlo Park, CA), was used in this study. The apparent molecular weight of STb thus obtained is expected at ~6.6 kDa by the addition of 6 amino acids (glycine) as a linker as well as 6xHis-tag at the C-terminus (Figure 1). The WT *sTb* was cloned between *SnpI* sites and the fragment was linked to the His-tag sequence by a six-glycine linker at the C-terminal of the *STb* gene product. Mutations in this WT construct were created by a site directed mutagenesis according to the manufacturer's recommendations of Q5 high fidelity polymerase kit from New England Biolabs. *E. coli* BL-21 were transformed by heat-shock. Clones were screened by PCR and positive clones were sequenced by The Center for Applied Genomic (TCAG DNA Sequencing Facility, Sick Kids Hospital, Toronto, Canada).

2.4. Site-directed mutagenesis

The mutations were generated by site-directed mutagenesis and were designed to increase the GC ratio in the signal peptide mRNA sequence without any effect on the amino acids sequence. All silent mutations were generated by site-directed mutagenesis. Mutants S-I, S-II, and S-III were constructed as silent mutants with the third nucleotide in the codons were changed from an A/T to G/C to change the AU richness within the 5' end of the mRNA that codes for the signal sequence. The NS-I mutant was designed to replace the second and the third amino acids (Lys) with Arg as well as increasing the GC content. The NS-II was designed to create an effect on the secondary structure of the mRNA as well as the hydrophobic region. Thus, a hydrophobic amino acid was replaced with a charged amino acid (Leucine at position 8 was replaced with Arginine). All non-silent mutations were generated by site directed mutagenesis. The Q5® Site-Directed Mutagenesis Kit was purchased from New England Biolabs and followed the recommended instructions for the PCR reactions.

2.5. Subcellular fractionation

Localization of expressed STb constructs was followed in three cellular fractions: culture supernatant (secreted), osmotic shock (periplasmic), and cytosolic. The supernatant fractions were collected by removal of cells through centrifugation at 5,000 xg for 10 min. The collected cells were then subjected to osmotic shock according to the protocol of Heppel, L.A. [18] with some modification. Briefly, the washed cells were suspended in minimal volume of 25 mM Tris, pH 7.4 containing 1 mM EDTA and 20% sucrose and incubated on ice for 30 min. The cells were then collected and resuspended in 5.0 ml of cold $MgCl_2$ solution (0.5 mM) and incubated on ice for an additional 20 min. The treated cells were finally centrifuged at 14,000 xg for 30 min. The supernatant, representing the osmotic shock, was collected and the pellet was used to prepare the cytosolic fractions. Treated cells were

Figure 1. The primary structure of STb and the mutations constructed within the N-terminal signal sequence. (A) The amino acid sequence of STb showing its signal sequence as the N-terminal 23 amino acid residues and the signal peptidase cleavage site at Ala 23 (arrow). (B) The mRNA sequences of the signal sequence in the WT and the mutants S-I, S-II, S-III, NS-I, and NS-II. Boxed nucleotides outline the changes in the WT mRNA sequence in the mutant constructs.

resuspended in 5.0 ml of cold TBS containing 1 mM EDTA and subjected to 10 cycles of ultrasonic bursts at 16 V using a W208 Sonicator (Heat Systems UltraSonic Inc.) equipped with a micro-tip. Each cycle consisted of 5 s ON followed by a 30 s rest on ice. The resulting suspension was centrifuged at 14,000 xg for 30 min. The resulting supernatant was used as the cytosolic fraction.

2.6. Tricine-SDS-PAGE and western blots

Tricine Sodium dodecyl sulfate-polyacrylamide gel electrophoresis (Tricine-SDS-PAGE) gels were used to detect STb because of its small size. 16% SDS-PAGE gels were prepared as recommended by Schagger [19]. Following electrophoresis, the proteins were transferred to a Polyvinylidene fluoride (PVDF) membrane and developed with mouse anti-6xHis antibodies followed by goat anti-mouse IgG-horseradish peroxidase antibody conjugate [GenScript, lot #A109704] for one hour at ambient temperature. Then the membrane was washed three times with PBS, developed using chemiluminescence substrate [Bio-RAD, USA], and visualized using a Chemidoc XRS [Bio-RAD, USA] documentation system.

2.7. Acid phosphatase assay

Acid phosphatase activity in the subcellular fractions were evaluated using p-nitrophenyl phosphate (*p*-NPP) as substrate at pH 4.0 according to a previous protocol [20] and using a microtitre plate format. Briefly, 200 µl reactions were set up containing acetate buffer (40 mM, pH 4.0), *p*-NPP (2 mM), and 10 µg of protein extracts. Reactions were incubated at ambient temperature for 2 h followed by addition of 50 µl of 5N NaOH. Released *p*-NP was then measured at 405 nm in a microplate reader (GeneSpec III spectrophotometer, Hitachi Genetic Systems, San Francisco, CA).

2.8. STb quantification

Secreted STb was quantified using a competitive ELISA assay. The His-Tag ELISA Detection Kit [GenScript, lot no. L00436] was used according to the recommended protocol of the manufacturer.

2.9. mRNA quantification

The samples were prepared by transferring about 2×10^9 to 2×10^{10} cells into 1.5 ml eppendorf tube from a logarithmic growth culture. Centrifuged at 12,000 xg for 30s using AccuSpin™ Micro [Fisher Scientific, Germany] and discarded the supernatant. Then the cells were suspended thoroughly in 100µl of a fresh Lysozyme solution (400 µg/ml in RNase-free water) and incubated at 37 °C for 5 min. After that RNase-free pipette filtered tips were used to add 1 ml of lysis buffer (Buffer-B) and mixed gently by inverting then incubated at room temperature for 5 min. A 200 µl of chloroform was added to each sample and mixed by inverting. Then the samples were centrifuged at 12,000 xg for 5 min at 4 °C using AccuSpin™ Micro [Fisher Scientific, Germany] and the supernatants were transferred to a new RNase-free 1.5 ml eppendorf tube. A 200 µl of ethanol 100% was added to each sample and vortexed for 30 s then incubated at -80 °C for 45 min for a higher RNA yield. After the samples were centrifuged at 12,000 xg for 5 min at 4 °C using AccuSpin™ Micro [Fisher Scientific, Germany] and discarded the supernatants carefully. Then the pellets were washed with RNase-free 75% ethanol twice by inverting for 10 times. After the samples were spun at 12,000 xg for 1 min using AccuSpin™ Micro [Fisher Scientific, Germany], discarded the supernatant and air-dried the pellet for 15 min at room temperature. Finally, 30 µl of RNase-free water was added to dissolve each RNA pellet and stored at -80 °C for long term storage. Then 1.0 µl of total RNA extraction was resuspended in 499 µl of RNase-free water in 0.5ml quartz cuvette to be quantified using a Shimadzu UV-2401PC Spectrophotometer (Hitachi, Japan).

2.10. Quantitative RT-PCR

The rapid bacterial RNA isolation kit [Bio-Basic Inc.] was used to isolate total RNA. For the qRT-PCR, the reactions were carried out using in The Chromo4 Real Time PCR Thermocycler [Bio-Rad, USA] and according to the recommended protocol of 2x QuantiTect SYBR Green PCR kit [Qiagen]. Primer pairs were designed computationally using Primer-BLAST web-Sever based on 50 °*C* minimum and 65 °*C* maximum melting temperature with a 3° maximum difference between each pair to create 70bp to 180bp products and synthesised by Invitrogen (Table S2). As an internal standard, the 16S rRNA was used (Table S2).

2.11. Statistical analysis

Unless otherwise stated, error bars in the Figures represent standard error of the means. Values were compared by one-way ANOVA. $P < 0.05$ was considered significant.

3. Results

3.1. mRNA secondary structure simulations

Single-stranded RNA forms secondary structures through the interactions of complementary segments. These secondary structures may influence many cellular processes, including mRNA stability and localization, transcription, RNA processing, and translation (18, 19). To assist with the analysis of our experimental observations, simulations of the secondary structures were carried out for the WT and the mutant STb mRNA transcripts. A previous computational study proposed a possible specific recognition and mediating role in targeting secreted protein for secretion via the T2SS by the AU richness of the mRNA sequence within the 5′ end of the molecule (8). The study concluded that secretion efficiency increases with higher AU richness. In this work the AU richness in the first 69 nucleotides of the STb mRNA was decreased step-wise by constructing three mutants, S-I, S-II, and S-III. Two additional mutants, NS-I and NS-II, were constructed as controls (Table 1). The simulations were carried out on the STb mRNA transcripts including 29 nt upstream of the start codon (5′ UTR).

The signal sequence of the STb is composed of the 23 N-terminal amino acids (Figure 1). The mutations in this study were contained within the first 23 codons of the transcripts. From the simulations (Figure 2), it was observed that a stem-loop structure between nt 100–130 is present in all 6 transcripts used in this study. This sequence falls within the N-terminal region of the mature STb protein and after the cleavage site of the signal sequence. Mutant construct S-II shows an additional stem-loop structure between nt 36–50 (Figure 2B), which falls within the mutated 5′ coding sequence of STb. The limited non-silent mutations in the NS-I and NS-II do not appear to impact the secondary structure in any significant way (Figure 2C). The structures have minimum free energies (MFE) similar to that of the WT STb (E = -46 Kcal/mol) and similar overall folding. The silent mutations in constructs S-I, S-II, and S-III had more pronounced effects on the other hand. The overall structures of these constructs were significantly different than that of WT STb and different MFEs. The MFE of S-I construct is -51.6, increased to -56.1 for S-II construct, and further to -62.1 for construct S-III. This is consistent with the gradual increase in the GC content in the mutated 5′ coding region of STb mRNA (Figure 1).

3.2. Mutant clones secrete different levels of STb

Proteins in the cytosolic, periplasmic, and supernatant fractions were separated using SDS-Tricine gels and replica western blots developed with anti-6xHis tag were used to assess qualitatively the relative amounts of STb in those fractions. In addition to quantifying STb in the culture supernatant, it was also quantified in two other subcellular fractions, the periplasmic and the cytoplasmic fractions. The fractionation procedure

Table 1. Summary of observed effects of mutations on secretion of WT and mutant STb constructs.

Construct	AU/GC	A.A. mutation	Secreted STb	mRNA level	Growth	Secretion Efficiency
WT	2.13	–	1.00	1.00	1.00	1
S-I	1.65	–	0.88	1.25	1.02	0.70
S-II	1.30	–	0.06	3.21	1.02	0.02
S-III	0.97	–	0.75	1.01	1.00	0.75
NS-I	1.55	K2→R2 K3→R3	0.94	0.58	0.95	1.62
NS-II	2.00	L8→R8	0.02	4.49	0.51	0.002

Values in columns 4–7 are presented as relative values to those of WT.

was evaluated by measuring the relative amount of acid phosphatase activity. Presence of STb was evident in the culture supernatant but absent from the other subcellular fractions (data not shown). It appears to have a very short periplasmic transit time. Variations in STb levels in the culture supernatant is also evident in the various constructs. A competitive ELISA assay was used to quantify the relative levels of STb secreted by the WT and the mutant clones (Figure 3). Lowest levels were observed in mutants S-II and NS-II. Reducing AU richness (expressed as the fraction AU/GC) from 2.13 to 1.65 in S-I mutant resulted in a 12% decrease in secretion of STb (Figure 3, Table 1). Reducing the AU richness further to 1.3 in S-II mutant reduced secretion levels of STb to only 6% of the WT control. Curiously, the third mutant construct (S-III) with an AU richness of 0.97 displayed recovery of secretion to 75% of the WT control. The non-silent mutations in NS-I converted the 2 Lys at positions 2 and 3 to Arg, a change that would not be expected to impact the structure of the signal peptide and as shown in Figure 3 and Table 1, secretion of this mutant was comparable to that of the WT (94%). This was included as a control and an additional control, NS-II, show that changes to the signal peptide's basic structural organization (charged N-terminus and hydrophobic domain) can affect secretion of the target protein. In NS-II, the hydrophobic domain is interrupted by a positive charge from Arg at position 8 in place of Leu. In this case, secretion of STb was abolished (2%).

3.3. STb mRNA levels are affected by changes in AU richness

Levels of secreted proteins in general can be regulated at the level of transcription, mRNA stability (half-life), translation initiation

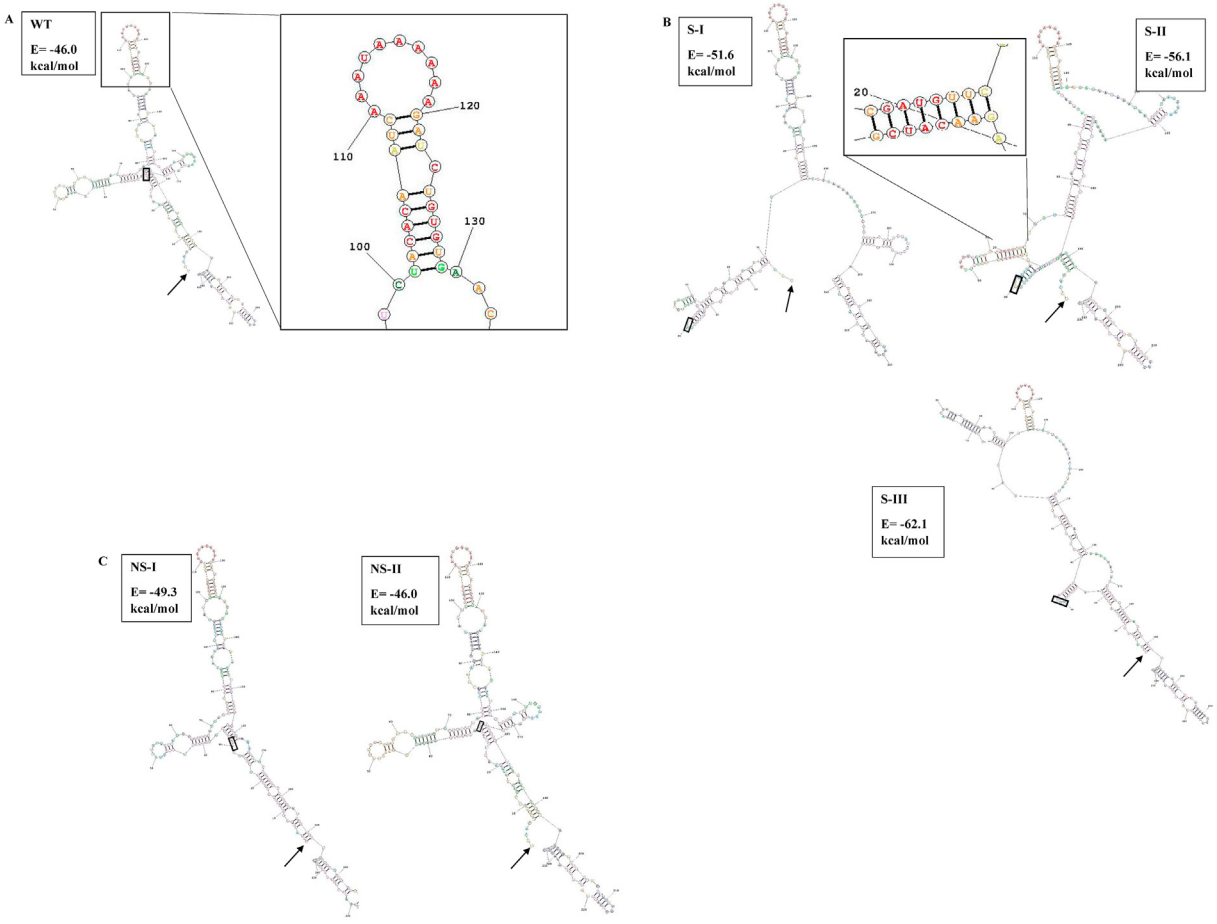

Figure 2. Simulations of mRNA fold using RNAstructure. The entire STb transcript was used in the simulations, including 29 nucleotides upstream of the start codon. The 5′ end of each transcript is identified by the arrow and the AUG start codon is boxed starting with nucleotide 30. (A) WT, (B) S-I, S-II and S-III, (C) NS-I and NS-II. Colours reflect base pairing probabilities (red ≥ 99%, Orange ≥95%, Yellow ≥90%).

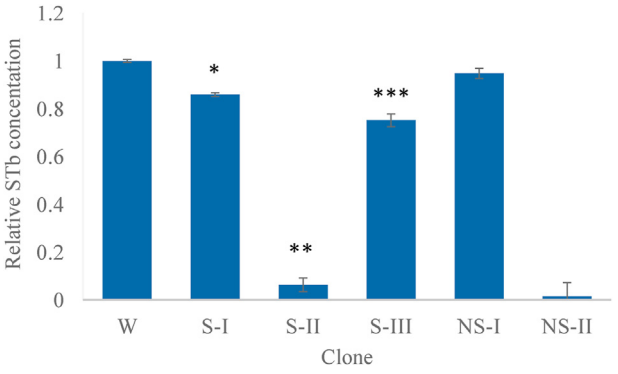

Figure 3. Competitive ELISA for secreted STb in culture media of STb clones. Values shown are relative to that of WT STb. Culture supernatants were normalized for protein concentration before the ELISA assay. The error bars represent the variations of five triplicates. The statistical results of One-Way ANOVA showed a significant difference compared to WT with *p*-value of <0.001. The post hoc test was done using Tukey test.

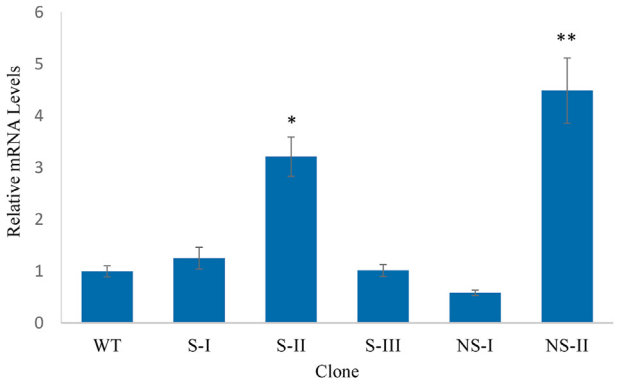

Figure 5. Abundance of mRNA transcripts for the WT and mutant constructs. Following induction of expression, total mRNA was extracted from the cells and subjected to qRT-PCR using the primers identified in Table S2. The relative abundance of mutant STb mRNA to that of WT is shown in the figure. Asterisks denote statistical significance ($p < 0.05$) with respect to the WT. Assay was repeated three times.

(mRNA-ribosome complex formation), rate of translation on the ribosome, and rate of processing through the Sec translocon and outer membrane. The STb constructs used in this study were under an inducible promoter, thus, we may exclude transcription as being involved in the changes in STb secretion observed in this study. The levels of mRNA transcripts of the WT were compared to the mutant constructs in order to uncover possible points of interruptions in this process. What we observed was an inverse correlation between the levels of secreted STb and the levels of STb mRNA. Going from high AU richness for the WT to low AU richness in S-I and S-II, secretion levels were lower (Figure 3) but mRNA levels increased (Figure 5). In the S-III mutant however, where the AU richness was further reduced in the mRNA, toxin secretion level was comparable with that of S-I instead of declining below the levels of S-II. The mRNA level of this mutant was also comparable to that of the WT construct. The NS-I mutant, in which the N-terminal Lys was converted to Arg, did not show significant effects on secretion or mRNA levels, observations that were anticipated. Production and secretion of the mature toxin was almost negligible in the NS-II mutant, a result that was also anticipated as the signal sequence was modified with a positive charge within the hydrophobic domain. Accumulation of the mRNA transcript for this construct was the highest of all constructs (Figure 5). Furthermore, the host BL21 for this construct displayed general growth retardation effects as compared to all other constructs (Figure 6). One may speculate that this growth retardation can be caused by the documented accumulation of the NS-II mRNA, possibly causing toxic effects and general growth retardation. This accumulation could be due to 'pausing' and incomplete translation of the NS-II mRNA caused by buildup of STb protein.

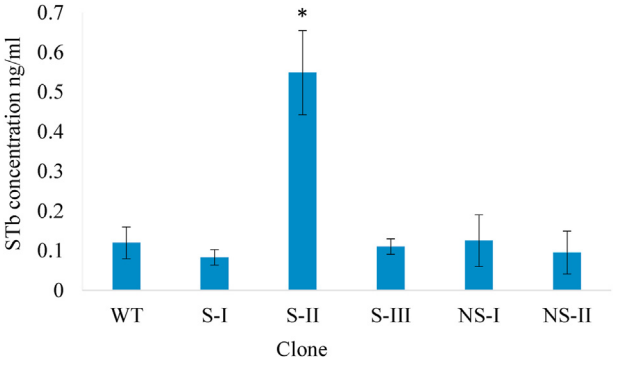

Figure 4. Levels of STb in the cytoplasmic fraction of cells following induction of expression. Stb levels were quantified using anti-6xHis antibodies in an ELISA assay. The data shown represent the averages of three analyses and the asterisk represents statistical significance at $p < 0.05$ (for each value with respect to WT).

3.4. STb accumulates in the cytoplasm in the S-II mutant

To define the exact step that caused the defect in the observed secretion of STb in S-II mutant, an analysis of the levels of STb in the cytoplasmic fraction was carried out. The results showed a clear accumulation of STb in the cytoplasmic fraction of the S-II mutant (Figure 4). The WT and all other constructs showed comparable levels of STb in this fraction. In contrast, the NS-II mutant, which showed a clear accumulation of its mRNA in this fraction (Figure 5), showed comparable levels of STb to the WT.

4. Discussion

The *E. coli* STb is a small polypeptide composed of 72 amino acids. It contains a prototypical T2SS signal in the first 23 residues ending in an AYA cleavage site. This signal sequence is cleaved off following translocation across the cytoplasmic membrane and the mature toxin, 49 residues long, is released to the extracellular milieu. This study was designed to examine the effect of modification of the AU richness level within the STb mRNA 5′ region (corresponding to the translated signal sequence) on secretion in the native host of the toxin. A number of silent mutations were introduced to reduce the AU richness in three stages: (1) in S-I construct codons at positions 2, 4, 6 and 7 were modified, (2) in S-II construct the same codons as in S-I construct plus codons 8–11, 14 and 15, were modified, and (3) in S-III construct the same codons as S-II plus codons 16–20, 22 and 23 were modified. All mutations involved changing the A/U at position 3 in each codon with G/C. As positive controls, two additional constructs were generated, NS-I in which the codons at positions 2and 3 (coding for Lys) were changed to codons for Arg, and NS-II in which the amino acid Leu at position 8 was replaced with the charged amino acid Arg. The results from the two positive controls validated our experimental approach and provided anticipated results. The mutations in NS-I did not change the basic structure of the signal sequence (positively charged N-terminus remains) and the secretion levels observed for this construct were slightly lower than that of the WT construct (88% compared to WT, Table 1).

The silent mutations in the S-I, S-II, and S-III constructs did not modify the primary structure of the signal sequence of the toxin but some interesting results were obtained, particularly with S-II and S-III constructs. Mutations in S-I caused a reduction of secretion of STb by

approximately 12% that of the WT (Figure 3). A corresponding increase in mRNA levels were observed for this construct (Figure 5). Since the signal sequence of the toxin was not modified in any way the insertion of this sequence within the Sec translocon is not expected to be affected as in the NS-II mutant construct. Since the mRNA levels were elevated it points to an inefficient translation as a possible cause for the observed effects. For our purposes, translation efficiency here is referred to the ability of the cell to process and translate the mRNA and can be evaluated by looking at the ratio of mRNA concentration and its protein product concentration, normalized to the values in the WT STb construct. Further reduction in the AU richness in S-II produced compounded effect. Secretion of this construct was severely reduced, down to about 6% of that of the WT STb construct (Figure 3). As in S-I, a corresponding build-up in S-II mRNA was observed (Figure 5). Here again inefficient translation, and not secretion itself, is a possible cause for the observed reduction in mRNA translation and secretion of the toxin. Examination of the secondary structure simulation (Figure 2B) show that this construct has an additional stem-loop structure within the 5′ coding region affected by the mutations (nt 36–50, codons 3–7), and an increase in the MFE value in comparison to the WT and the S-II STb constructs. The change in MFE calculations was expected as we increased the GC content beyond those changes in the S-II construct. These differences may explain the decreased efficiency of mRNA translation observed for this construct. Further reduction of AU richness in S-III however complicated the picture. Instead of further reduction in secretion a rebound of secretion efficiency was observed. This construct provided a secretion level equivalent to about 75% of that of the WT STb (Figure 3). The mRNA level of this construct was accordingly reduced (Figure 5), indicating that the translation and subsequent secretion of the toxin has recovered. This was surprising given that the calculated MFE value for this construct was higher than those of S-I and S-II constructs (-62.1 Kcal/mol compared to -51.6 Kcal/mol and -56.1 Kcal/mol, respectively). Energy calculations alone, however, do not necessarily correlate with translation efficiency [22, 23]. The secondary structure simulations also show that the stem-loop structure predicted in S-II between nucleotides 36–50 is released in the S-III construct (Figure 2B). This may explain the recovery of secretion in this construct even with further reduction of AU richness.

Codon abundance, tRNA abundance, or susceptibility to endonuclease attack of the mRNA are factors that also need to be considered.

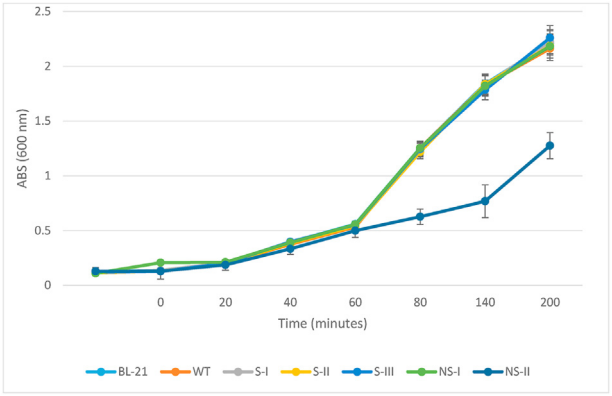

Figure 6. Growth curves for *E. coli* BL-21 expressing WT STb, and clones containing the various mutations. The graph shows growth retardation in the mutant construct NS-II.

However, analysis of our data reveals that such effects cannot explain our observations with S-I and S-II. The secondary structure of the mRNA and endonuclease susceptibility are unlikely causes of such effects because in S-I and S-II the mutations are accumulative (Figure 6). Reduced susceptibility of an mRNA to endonuclease attack would mean accumulation of mRNA but will not be expected to reduce the levels of secreted toxin in comparison to the WT STb, and this was not observed in our study. Codon and tRNA abundance effects due to the mutations that were introduced in the constructs are summarized in Table 2. In S-I, all the mutations were generated at position 3 (wobble position) and all four modified codons pair with the same tRNA, negating possible codon and tRNA abundance as possible causes for the observed reduced secretion. In this construct the codon modifications result in a net gain of 1 Watson·Crick (W·C) pairing. It is recognized that W·C pairing promotes more efficient translation whereas wobble pairing slows it down [7]. In S-I one would expect an enhancement rather than a reduction in translation and secretion. This is also the case for S-II, where there is a net gain of 2 W·C pairing as compared to the WT construct but instead, translation and secretion was almost abolished. This supports our analysis above, attributing the observed effects to changes in the secondary structure of

Table 2. Summary of codon change effects in mutant constructs on codon and tRNA abundance as well as effects on wobble pairing.

Clone	Codon #	WT codon	Mutant codon	Δ tRNA Abundance[1]	Δ in pairing[2]	Overall change
S-I	2	AAA	AAG	0	W·C → Wbl	+1 W·C pairing
	4	AAU	AAC	0	Wbl → W·C	
	6	GCA	GCG	0	Wbl → Wbl	
	7	UUU	UUC	0	Wbl →W·C	
S-II	8	CUU	CUG	+3.87	Wbl → Wbl	+2 W·C pairing
	9	CUU	CUG	+3.87	Wbl → Wbl	
	10	GCA	GCG	0	Wbl → Wbl	
	11	UCU	UCG	0	Wbl → Wbl	
	14	GUU	GUG	0	Wbl → Wbl	
	15	UUU	UUC	0	Wbl → W·C	
S-III	16	UCU	UCG	0	Wbl → Wbl	+3 W·C pairing
	17	AUU	AUC	0	Wbl → W·C	
	18	GCU	GCG	0	W·C → Wbl	
	19	ACA	ACG	0	W·C → Wbl	
	20	AAU	AAC	0	Wbl → W·C	
	22	UAU	UAC	0	Wbl → W·C	
	23	GCA	GCG	0	Wbl → Wbl	

S-II and S-III mutants accumulate the nucleotide changes presented by S-I and S-I/S-II, respectively, as showed in the Figure 1.

[1] change in abundance is calculated as: mutant codon abundance x new tRNA abundance/WT codon abundance x WT tRNA abundance. Where the same tRNA is used for both codons (mutant and WT), the change is given a value of zero.

[2] Change in pairing reflects the change in codon pairing (at the third nucleotide position) with cognate tRNA. Watson·Crick pairing is presented as W·C and wobble pairing is presented as Wbl.

the transcripts. Changes to codons 8 and 9 in S-II produced codons and tRNAs with higher abundance (Table 2), but toxin secretion was reduced, nonetheless. This is supported by the results shown in Figure 4, where STb accumulates in the cytoplasm. In the S-III construct, a net gain of 5 W·C pairings with no effect on codon/tRNA abundance was introduced. This, possibly combined with the release of the stem-loop structure between nt 36–50 introduced in S-II, could explain the rebound in translation/secretion efficiency of this construct. Secretion of both S-II and NS-II constructs were reduced but the cytoplasmic accumulation of NS-II was similar to that of WT STb (Figure 4). This was expected because in NS-II construct translation on the ribosome should not have been affected (insignificant change to the mRNA compared to WT). This means that this mutant STb will be produced in the cytoplasm at a comparable rate to that of WT STb and the cytoplasmic fraction would be expected to have comparable levels of STb protein. In the S-II construct, the changes in the mRNA were more significant and AU richness was changed to a level such that its translation was affected, thus increasing the amount of STb in the cytoplasmic fraction. A possible explanation for this effect could be the increased stability, and therefore half-life, of the S-II mRNA (Figure 5). This increased stability in the mRNA can then be translated into increased levels of STb in the cytoplasm.

In *E. coli*, there are 8 rare codons (CUA, UCC, UCA, CCU, CCC, CCA, ACA, and AGG) and 2 codons limited by their tRNA levels (UUA and GUC) (9). None of these codons were used in the constructs. Formation of the mRNA-ribosome complex and initiation of translation is another mechanism for control of translation. In *E. coli*, this process involves mRNA regions upstream of the start codon, a region of the mRNA that was not altered in our constructs. Within the coding region of the mRNA downstream of the start codon, AU richness may still enhance translation. Codons ending in G/C give higher folding energies than codons ending in A/U [7]. According to this effect, the reduced secretion efficiency observed for S-I and S-II due to reduction of AU richness can be explained. This, combined with the stem-loop structure in S-II may explain the severe reduction of secretion observed in our study. The factors involved in regulating translation differ somewhat between those proteins that are translated and fold within the cytoplasm from those that are translocated across the membrane in a co-translational process. This has been shown to be the case for slow-translating segments in Tat substrates as compared with Sec substrates [9, 10, 11]. Since it is highly unlikely that the insertion of the signal sequence of STb into the Sec translocon to be the cause of the observed decrease in secretion (the signal sequence was not altered), it leaves two possibilities: either the changes to the codons produced slow-translating segments or the initiation of the mRNA-ribosome complex was affected. Slow-translating segments involve segments of the mRNA where rare codons are present [9]. This is not the case in the constructs used in this study and one therefore may eliminate this possibility. This leaves the latter, mRNA-ribosome complex formation, as a possible step in the process of translation where the changes in AU richness produced their effect. This analysis is consistent with observations of Brock et al. [24] where downstream adenines influence expression through their effects on mRNA-ribosome association rates. The rebound in secretion of the S-III constructs maybe explained by the possibility that codon changes beyond codon 15 has shifted secondary structure elements away from the start codon, thus recovering the efficiency of mRNA-ribosome complex formation.

5. Conclusions

As a model substrate of the T2SS the *E. coli* STb was used to determine the effects of AU richness within the 5′ coding region of the mRNA. A series of mutations were created within the 5′-end of the STb mRNA (a region of 69 nucleotides) that corresponds to the 23 amino acid signal sequence for the T2SS. Converting the N-terminal pair of Lys to Arg showed no significant effect on the levels of secreted STb. A more significant mutation however, whereby the Leu at position 8 was converted to Arg, essentially abolished secretion of STb. This result was anticipated as the positive charge on Arg at position 8 disrupts the hydrophobic domain of the signal peptide and potentially pauses the secretion process during the membrane insertion step within the Sec translocon. Significantly, sequential decrease in the AU richness within the first 15 codons showed sequential decrease in the levels of secreted STb. These mutations were silent and did not alter the identity of the amino acid signal sequence of the toxin. Reduction in AU richness beyond the first 15 codons reverted secretion levels of the toxin. Codon and tRNA abundance was excluded as possible causes for the observed effects. Secondary structure of the constructs and possibly the mRNA-ribosome association rates may explain the effects of AU richness observed in our study, although the latter was not specifically examined in this study. These results indicate the importance of AU richness within the 5′coding region of the mRNA in secretion efficiency but also point to the role of other factors, such as stem-loop structures. The results in this work can also be of value in both homologous and heterologous expression of STb.

Declarations

Author contribution statement

E. Kinkar: Conceived and designed the experiments; Performed the experiments; Analyzed and interpreted the data; Wrote the paper.

A. Kinkar: Analyzed and interpreted the data.

M. Saleh: Conceived and designed the experiments; Analyzed and interpreted the data; Contributed reagents, materials, analysis tools or data; Wrote the paper.

Funding statement

This work was supported by the Laurentian University Research Fund.

Competing interest statement

The authors declare no conflict of interest.

Additional information

Supplementary content related to this article has been published online at https://doi.org/10.1016/j.heliyon.2020.e05330.

Acknowledgements

We wish to thank Dr. Paul Michael for his assistance with instrumentation.

References

[1] C.Y. Chen, J.G. Belasco, Degradation of pufLMX mRNA in Rhodobacter capsulatus is initiated by nonrandom endonucleolytic cleavage, J. Bacteriol. 172 (8) (1990) 4578–4586.

[2] D. Bechhofer, 5′ mRNA stabilizers, p. 31–52, in: J.G. Belasco, G. Brawerman (Eds.), Control of Messenger RNA Stability, Academic Press, Inc., San Diego, CA, 1993.

[3] C.F. Higgins, H.C. Causton, G.S.C. Dance, E.A. Mudd, The role of the 3′ end in mRNA stability and decay, p. 13–30, in: J.G. Belasco, G. Brawerman (Eds.), Control of Messenger RNA Stability, Academic Press, Inc., San Diego, CA, 1993.

[4] S. Altuvia, A. Zhang, L. Argaman, A. Tiwari, G. Storz, The *Escherichia coli* OxyS regulatory RNA represses fhlA translation by blocking ribosome binding, EMBO J. 17 (1998) 6069–6075.

[5] R.A. Lease, M.E. Cusick, M. Belfort, Riboregulation in *Escherichia coli*: DsrA RNA acts by RNA: RNA interactions at multiple loci, Proc. Natl. Acad. Sci. USA 95 (1998) 12456–12461.

[6] C.S. Baker, I. Morozov, K. Suzuki, T. Romeo, P. Babitzke, CsrA regulates glycogen biosynthesis by preventing translation of glgC in *Escherichia coli*, Mol. Microbiol. 44 (2002) 1599–1610.

[7] G. Boël, R. Letso, H. Neely, W.N. Price, K.H. Wong, M. Su, R. Xiao, Codon influence on protein expression in *E. coli* correlates with mRNA levels, Nature 529 (2016) 358.
[8] N.T. Ingolia, L.F. Lareau, J.S. Weissman, Ribosome profiling of mouse embryonic stem cells reveals the complexity and dynamics of mammalian proteomes, Cell 147 (2011) 789–802.
[9] G. Zhang, M. Hubalewska, Z. Ignatova, Transient ribosomal attenuation coordinates protein synthesis and co-translational folding, Nat. Struct. Mol. Biol. 16 (2009) 274–280.
[10] B.C. Berks, T. Palmer, F. Sargent, Protein targeting by the bacterial twin-arginine translocation (Tat) pathway, Curr. Opin. Microbiol. 8 (2005) 174–181.
[11] A.J. Driessen, N. Nouwen, Protein translocation across the bacterial cytoplasmic membrane, Annu. Rev. Biochem. 77 (2008) 643–667.
[12] V. Vimberg, A. Tats, M. Remm, T. Tenson, Translation initiation region sequence preferences in Escherichia coli, BMC Genom. 8 (2007) 100.
[13] A.V. Komarova, L.S. Tchufistova, M. Dreyfus, I.V. Boni, AU-rich sequences within 5′ untranslated leaders enhance translation and stabilize mRNA in Escherichia coli, J. Bacteriol. 187 (2005) 1344–1349.
[14] Anders Aamann Rasmussen, Maiken Eriksen, Kambiz Gilany, Christina Udesen, Thomas Franch, Carsten Petersen, Poul Valentin-Hansen, Regulation of ompA mRNA stability: the role of a small regulatory RNA in groWTh phase-dependent control, Mol. Microbiol. 58 (2005) 1421–1429.
[15] K. Yamagishi, T. Oshima, Y. Masuda, T. Ara, S. Kanaya, et al., Conservation of translation initiation sites based on dinucleotide frequency and codon usage in Escherichia coli K-12 (W3110): non-random distribution of A/T-rich sequences immediately upstream of the translation initiation codon, DNA Res. 9 (2002) 19–24.
[16] D.M. Anderson, O. Schneewind, *Yersinia enterocolitica* T3SS secretion: an mRNA signal that couples translation and secretion of YopQ, Mol. Microbiol. 31 (1999) 1139–1148.
[17] D.H. Mathews, M.D. Disney, J.L. Childs, S.J. Schroeder, M. Zuker, D.H. Turner, Incorporating chemical modification constraints into a dynamic programming algorithm for prediction of RNA secondary structure, Proc. Natl. Acad. Sci. Unit. States Am. 101 (2004) 7287–7292.
[18] L.A. Heppel, The effect of osmotic shock on release of bacterial proteins and on active transport, J. Gen. Physiol. 54 (1969) 95–113.
[19] H. Schägger, Tricine-SDS-PAGE, Nat. Protoc. 1 (2006) 16.
[20] M.T. Saleh, J.T. Belisle, Secretion of an acid phosphatase (SapM) by *Mycobacterium tuberculosis* that is similar to eukaryotic acid phosphatases, J. Bacteriol. 182 (2000) 6850–6853.
[22] P. Somogyi, A.J. Jenner, I. Brierley, S.C. Inglis, Ribosomal pausing during translation of an RNA pseudoknot, Mol. Cell Biol. 13 (1993) 6931–6940.
[23] M. Kozak, Influences of mRNA secondary structure on initiation by eukaryotic ribosomes, Proc. Natl. Acad. Sci. U.S.A. 83 (1986) 2850–2854.
[24] J.E. Brock, R.L. Paz, P. Cottle, G.R. Janssen, Naturally occurring adenines within mRNA coding sequences affect ribosome binding and expression in *Escherichia coli*, J. Bacteriol. 189 (2007) 501–510.